Intramolecular Energy Flow and Bond Dissociation in the Collision between Vibrationally Excited Toluene and HF

Jongbaik Ree,* Sung Hee Kim, Taeck Hong Lee,† and Yoo Hang Kim‡

*Department of Chemistry Education, Chonnam National University, Gwangju 500-757, Korea. *E-mail: jbree@chonnam.ac.kr*
†Department of Chemical Engineering, Hoseo University, Asan, Chungnam 336-795, Korea
‡Department of Chemistry and Center for Chemical Dynamics, Inha University, Incheon 402-751, Korea
Received November 2, 2005

Intramolecular energy flow and C-H_{methyl} and C-H_{ring} bond dissociations in vibrationally excited toluene in the collision with HF have been studied by use of classical trajectory procedures. The energy lost by the vibrationally excited toluene upon collision is not large and it increases slowly with increasing total vibrational energy content between 20,000 and 45,000 cm^{-1}. Above the energy content of 45,000 cm^{-1}, however, energy loss decreases. Furthermore, in the highly excited toluene, toluene gains energy from incident HF. The temperature dependence of energy loss is negligible between 200 and 400 K. Energy transfer to or from the excited methyl C-H bond occurs in strong collisions with HF transferring relatively large amount of its translational energy ($>>k_BT$) in a single step, whereas energy transfer to the ring C-H bond occurs in a series of small steps. When the total energy content E_T of toluene is sufficiently high, either C-H bond can dissociate. The C-H_{methyl} dissociation probability is higher than the C-H_{ring} dissociation probability. The dissociation of the ring C-H bond is not the result of the intermolecular energy flow from the direct collision between the ring C-H and HF but the intramolecular flow of energy from the methyl group to the ring C-H stretch. The C-H_{ring}···HF interaction is not important in transferring energy and in turn bond dissociation.

Key Words : Collision-induced, Intramolecular, Toluene, HF, Dissociation

Introduction

The collision-induced relaxation of vibrationally excited polyatomic molecules has been the subject of continuing interest in chemistry and physics for the past several decades.[1-11] Molecules vibrationally excited to near their dissociation threshold can undergo bond dissociation and vibrational relaxation, processes that play an important role in reaction dynamics. Recent studies[10-18] show that when the excited molecule is a large organic molecule, the average amount of energy transfer per collision is not very large. The average energy transfer per collision between the highly vibrationally excited benzene and a noble gas atom is known to be about 30 cm^{-1}, which is much smaller than benzene derivatives such as hexafluorobenzene or other hydrocarbons such as toluene and azulene.[6,8,19-22] For example, for hexafluorobenzene + Ar, the measured value of the mean energy transfer per collision by the ultraviolet absorption method is −330 cm^{-1},[20] whereas the calculated value using quasiclassical trajectory methods at 300 K is −150 cm^{-1}.[23] For toluene + Ar, the amount of energy transfer is about −200 cm^{-1}.[21] An important characteristic of vibrational relaxation in a large molecule is intramolecular energy flow, which plays the key role in bond dissociation. Among such large molecules, toluene is a particularly attractive molecule for studying collision-induced intramolecular energy flow and bond dissociation because of the presence of both methyl and ring CH bonds, presenting an intriguing competition among them. In elucidating this competition, it is particularly important to understand the direction of intramolecular energy flow in the interaction zone, *i.e.*, from the ring CH to the methyl CH or the reverse.

The purpose of this paper is to study the collision-induced dynamics of highly vibrationally excited toluene interacting with HF using quasiclassical trajectory calculations. Using the results obtained in the calculations, we discuss the time scale for bond dissociation, the relaxation of the excited CH vibration, and the time evolution of collision-induced intramolecular energy flow from the highly excited CH vibration. Finally, we elucidate the nature and mechanism of competition between methyl CH mode and ring CH mode in transferring energy to or from the incident molecule.

Interaction Model and Energies

The model for the toluene-HF interaction and vibrational coordinates of toluene are defined in Figure 1, where all carbon atoms, the ring hydrogen atoms and the incident molecule are assumed to be coplanar. In Figure 1a, we define all 39 intramolecular coordinates of the planar ring needed to be included in the present study. In Figure 1b, we define the interaction coordinates between the methyl CH bond and the adjacent ring CH bond of a non-rotating toluene with the incident HF molecule. The CH_{ring} bond is in the clockwise side from CH_{methyl}. We include 6 stretches (x_1, x_2, x_3, x_4, x_{14}, x_{15}) and 12 bends (ϕ_1, ϕ_2, ϕ_3, ϕ_4, ϕ_5, ϕ_6, ϕ_7, ϕ_1', ϕ_1'', ϕ_6, ϕ_6', ϕ_6'') in the interaction zone where the CH_{methyl} and CH_{ring} bonds are in direct interaction with HF. We then include the x_5-x_9 $(CC)_{ring}$ stretches, x_{10}-x_{13} $(CH)_{ring}$ stretches and ϕ_8-ϕ_{19} bends around the carbon atoms C_3, C_4, C_5 and C_6,

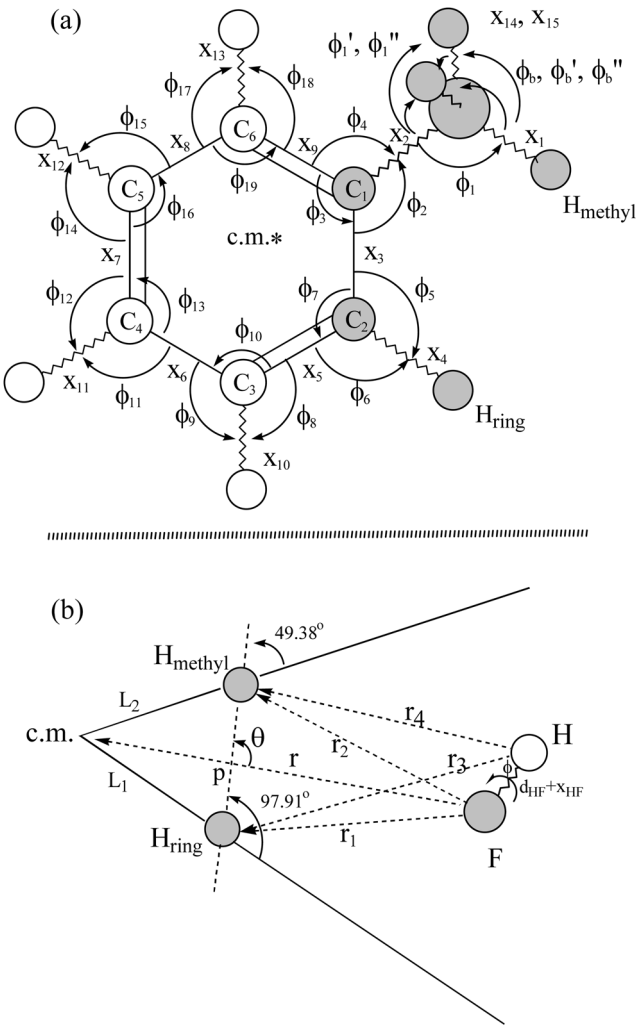

Figure 1. Collision model. (a) The stretching and bending coordinates of vibrations included in the model. All carbon atoms and ring H atoms are coplanar and modes are numbered clockwise. The star denotes the center-of-mass (cm) of toluene. For convenience we identify each vibration by its displacement (e.g., x_1 for $x_{e1} + x_1$). (b) The relative coordinate between HF and the cm of toluene (r), the F-to-H_{ring} distance (r_1), the F-to-H_{methyl} distance (r_2), H-to-H_{ring} distance (r_3) and H-to-H_{methyl} distance (r_4) are shown.

a total of 9 stretches and 12 bends, in the inner zone of the molecule.

The important step in developing an interaction potential model is to start with physically reasonable interaction potential energies, which are dependent on the pertinent collision coordinates. The interaction energies needed to describe the collision of HF with toluene must contain terms responsible for the coupling of the relative motion with the ring C-H stretch and methyl group C-H stretch as well as the coupling between the stretches and bends. We first introduce the interatomic distances r_1-r_4 in the interaction model defined in Figure 1b, where r represents the distance between c.m. of HF and the c.m. of toluene describing the relative motion of the collision system. The interatomic distances can be expressed in terms of the instantaneous coordinates of the C-H_{methyl} bond, C-CH_{methyl} bond, (C-C)$_{ring}$ bond, C-H_{ring} bond, CCH_{methyl} bend, CCC_{methyl} bend and CCH_{ring} bend. That is, $r_i = r_i$ (r, x_1, x_2, x_3, x_4, ϕ_1, ϕ_2, ϕ_5, x_{HF}, θ) for i = 1-4, where θ is the angle of incidence defined in Figure 1b. The coupling of these modes with others including those of the inner zone will have to be considered in formulating the overall interaction energy. The values of equilibrium bond distances and other potential parameters except HF are listed in Table I of Ref. 17. Each bond length will be denoted by ($x_{ei} + x_i$), where x_i is the displacement of the bond length from its equilibrium value x_{ei}. Similarly, we express each bending coordinate as ($\phi_{ej} + \phi_j$), where ϕ_j is the displacement of the jth bending vibration from the equilibrium angle ϕ_{ej}.

The F-to-H_{ring}(r_1), F-to-H_{methyl}(r_2), H-to-H_{ring}(r_3) and H-to-H_{methyl}(r_4) interatomic distances can be obtained as

$$r_1 = [y_1^2 + (d_{HF} + x_{HF})^2 \mu_H^2 - 2y_1(d_{HF} + x_{HF})\mu_H \cos(\phi - \rho_1)]^{1/2} \quad (1a)$$

$$r_2 = [y_2^2 + (d_{HF} + x_{HF})^2 \mu_H^2 - 2y_2(d_{HF} + x_{HF})\mu_H \cos(\phi - \rho_2)]^{1/2} \quad (1b)$$

$$r_3 = [y_1^2 + (d_{HF} + x_{HF})^2 \mu_F^2 - 2y_1(d_{HF} + x_{HF})\mu_F \cos(\pi - \phi - \rho_1)]^{1/2} \quad (1c)$$

$$r_4 = [y_2^2 + (d_{HF} + x_{HF})^2 \mu_F^2 - 2y_2(d_{HF} + x_{HF})\mu_F \cos(\pi - \phi - \rho_2)]^{1/2} \quad (1d)$$

where, ϕ is the rotational angle of HF, $\mu_H = m_H/(m_H + m_F)$, $\mu_F = m_F/(m_H + m_F)$, x_{HF} is the displacement of the HF from its equilibrium bond distance d_{HF}, and y_1 and y_2 are distances between H_{ring} and H_{methyl} and the c.m. of HF, respectively, and defined as

$$y_1 = [(r-z)^2 + A^2 - 2A(r-z)\cos\theta]^{1/2}, \quad (2a)$$

$$y_2 = [(r-z)^2 + B^2 - 2B(r-z)\cos\theta]^{1/2}, \quad (2b)$$

Here,

$$z = c_1\sin(97.91^\circ)/\sin\theta, \quad A = c_2\sin(\theta - 49.38^\circ)/\sin\theta,$$
$$B = c_1\sin(97.91^\circ - \theta)/\sin\theta$$

$$\rho_1 = \sin^{-1}\left[\frac{A}{r_1}\sin\theta\right], \quad \rho_2 = \sin^{-1}\left[\frac{B}{r_2}\sin(\pi-\theta)\right]$$

$$c_1 = [q^2 + (x_{e4} + x_4)^2 + 2q(x_{e4} + x_4)\cos(\phi_5 - \lambda/2 - \eta)]^{1/2},$$

$$c_2 = [G^2 + (x_{e1} + x_1)^2 - 2G(x_{e1} + x_1)\cos(107.6^\circ + \phi_1 - \xi)]^{1/2},$$

$$G = [0.8840 + (x_{e2} + x_2)^2 - 1.880(x_{e2} + x_2)\cos\phi_2]^{1/2},$$

$$q = [d^2 - 0.9096\, d\cos(60^\circ + \lambda) + 0.2068]^{1/2},\ d = 1.398\ \text{Å},$$

$$\xi = \sin^{-1}[0.9402\sin\phi_2/G],$$

$$\lambda = 2\sin^{-1}[x_3/(3^{1/2} d)],$$

$$\eta = \sin^{-1}[0.4548\sin(60^\circ + \lambda)/\theta].$$

Here all distances are in Å and z is distance between the c.m. of toluene and point "p" between H_{ring} and H_{methyl}.

The above distances and relations determine the coupling of the translation to vibrational motions (*i.e.*, the coupling of r with x_1, x_2, x_3, x_4, ϕ_1, ϕ_2, ϕ_5, and x_{HF}). These x's and ϕ's are then coupled with the inner modes indicated in Figure 1a.

The overall interaction energy is the sum of the Morse-type intermolecular terms, Morse-type stretching terms and the harmonic bending terms of toluene, intramolecular coupling terms, and Morse-type stretching term of HF,

$$V = \Sigma U(r_\alpha) + U_s(x_i) + U_b(\phi_j) + U_{int}(Y_iY_j) + U_{HF}(x_{HF}) \quad (3)$$

Where,

$$U(r_\alpha) = D[e^{(r_{e\alpha}-r_\alpha)/a} - 2e^{(r_{e\alpha}-r_\alpha)/2a}],\ \alpha = 1\text{–}4$$

$$U_s(x_i) = \Sigma D_i[1 - e^{-x_i/b_i}]^2,\ i = 1\text{–}15$$

$$U_b(\phi_j) = 1/2\Sigma k_j\phi_j^2,\ j = 1\text{–}24$$

$$U_{int}(Y_iY_j) = \sum_{ij} K_{ij}(Y_i - Y_{ei})(Y_j - Y_{ej}),\ i \neq j$$

$$U_{HF}(x_{HF}) = D_{HF}[1 - e^{-x_{HF}/b_{HF}}]^2.$$

For the intermolecular interaction, we take D = 379.9 k_B, the Lennard-Jones (LJ) parameter for the well depth for the collision pairs calculated by the usual combining rule,[24] where k_B is the Boltzmann constant, and a = 0.276 Å.[25] For the ith stretch, we use $b_i = (2D_i/\mu_i\omega_i^2)^{1/2}$, where $D_i = D_{o,i} + 1/2\ \omega_{ei}$, to determine the exponential range parameters listed in Table 1 of Ref. 17. The potential and spectroscopic constants for the HF are $D^0_{0,HF}$ = 5.869 eV and $\omega_{HF}/2\pi c$ = 4138.32 cm^{-1}.[26] The exponential range parameter b_{HF} is 0.225 Å determined from the relation $b_{HF} = (2D_{HF}/\mu_{HF})^{1/2}/\omega_{HF}$. The equilibrium distance of HF is d_{HF} = 0.968 Å.[27] In the coupling terms, $Y_i = x_i$ or ϕ_i and the coupling constant K_{ij} are taken from Xie and Boggs' ab initio calculations.[27]

In Figure 2, we present the equipotential plot of the overall interaction energy for HF approaching the molecule, which is in its equilibrium geometry. The molecule is oriented and scaled to closely represent the collision configuration and the center-of-mass of toluene is fixed at the origin of the plot. Here the abscissa is the c.m. of toluene to c.m. of HF line at θ = 90° and the ordinate, which is parallel to the

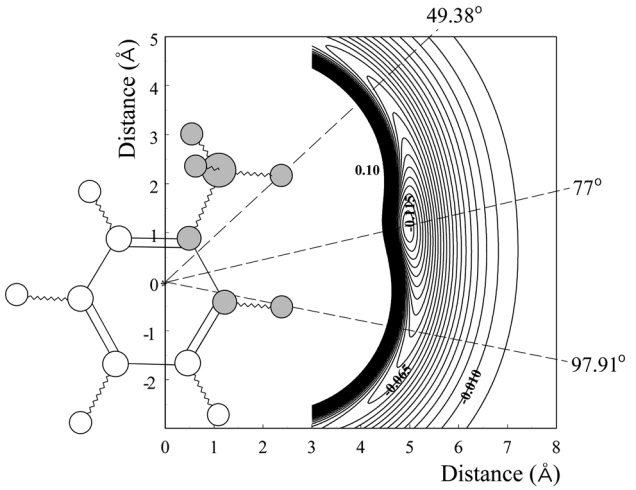

Figure 2. The equipotential plot of the interaction energy for HF interacting with C-H_{methyl} and C-H_{ring} of the fixed toluene from different direction. The origin (0,0) of the plot is the cm of toluene. The contours are labeled in electron volt and they are in 0.005 eV intervals. The repulsive region is truncated at 0.10 eV.

H_{methyl}-to-H_{ring} axis, passes through the c.m. of toluene. We note that the latter axis closely bisects the two C-C distances of the benzene ring perpendicularly as depicted in Figure 2. The intermolecular interaction energy surface exhibits a potential well along HF approaching the c.m. of toluene at the angle θ = 77°. The angle θ is measured from the line connecting the hydrogen atoms H_{methyl} and H_{ring} to the line connecting c.m. of HF and c.m. of toluene as shown in Figure 1. The potential minimum of 0.115 eV or 1020 k_B appears at r = 4.95 Å from the origin in the direction which lies in the intermediate region between the two hydrogen atoms. For r < 5 Å, the interaction energy rises rapidly and the contour lines (*i.e.*, above 0.10 eV) for this repulsive region is not shown in Figure 2.

The equations of motion which determine the time evolution of the relative motion (trajectory), 15 stretches and 24 bends for the given incident angle θ are

$$\mu d^2r(t)/dt^2 = -\frac{\partial}{\partial r} V(r, x_1,.., x_{15}, \phi_1,..., \phi_{24}, x_{HF}, \theta), \quad (3a)$$

$$\mu_i d^2x_i(t)/dt^2 = -\frac{\partial}{\partial x_i} V(r, x_1,.., x_{15}, \phi_1,..., \phi_{24}, x_{HF}, \theta),\ i = 1 - 15 \quad (3b)$$

$$I_j d^2\phi_j(t)/dt^2 = -\frac{\partial}{\partial \phi_j} V(r, x_1,.., x_{15}, \phi_1,..., \phi_{24}, x_{HF}, \theta),\ j = 1 - 24 \quad (3c)$$

$$\mu_{HF} d^2x_{HF}(t)/dt^2 = -\frac{\partial}{\partial x_{HF}} V(r, x_1,.., x_{15}, \phi_1,..., \phi_{24}, x_{HF}, \theta), \quad (3d)$$

where μ is the reduced mass of the collision system, μ_i is the reduced mass associated with the ith stretch and I_j is the moment of inertia of the jth bend. μ_{HF} is the reduced mass of HF. We use the standard numerical routines[28,29] to integrate these equations for the initial conditions at $t = t_0$ and their conjugate quantities $(d/dt)x(t_0)$, $(d/dt)x_i(t_0)$, $(d/dt)\phi_j(t_0)$, and $(d/dt)x_{HF}(t_0)$, where the derivatives are evaluated at $t = t_0$. In our calculations, we have already shown that the interaction near θ = 77° plays the dominant role in promoting energy loss or C-H bond dissociation through inter- or intra-molecular energy transfer.[11] Thus, in all collision systems considered here, the incident atom approaches the center of mass of toluene in the θ = 77° direction, where the CH_{methyl}-HF and CH_{ring}-HF interactions are very close to each other and where energy transfer is most efficient.[11]

Numerical Procedures

We solve the equations of motion for the relative motion, 15 stretches and 24 bends of toluene, and HF vibration using the DIVPAG double-precision routine of the IMSL library[28,29] to describe the time evolution of bond distances, bond angles, and vibrational energies, as well as the relative coordinate for the model system. We sample 40,000 trajectories for each run at 300 K, where the sampling includes determining collision energies (E) chosen from the Maxwell distribution. To study the temperature dependence of energy transfer, the calculation will also be carried out at T = 200

and 400 K. In studying the E dependence of energy transfer and bond dissociation, we carry out the same sampling except that E is now fixed at a specified value. The initial conditions for solving the equations of motion for the relative motion and the displacements and phases for the vibrational motions in the interaction zone are given in Ref. 11. We vary the initial vibrational energies of the C-H_{ring} and C-H_{methyl} bonds (*i.e.*, i = 1 and 4) systematically, while maintaining the rest of the vibrational motions in the ground state. Each vibrational phase is a random number $\delta_i = 2\pi s_i$ with flat distribution of s_i in the interval (0,1). The initial separation between the center of masses of toluene and HF is set as 15 Å, and trajectories are terminated when the separation reaches 50 Å after they passed through the closest distance of approach. The integration was performed with a stepsize of 0.169 fs, which is one-tenth the period of the largest frequency, the ring CH vibration, and is small enough to ensure energy conservation to at least five significant figures along a trajectory. We have also confirmed that the numerical procedure allows the trajectories to be successfully backintegrated.

For such highly excited CH vibrations considered here, the discussion of bond dissociation in terms of normal-mode analysis is not useful since the dissociation does not involve a particular normal mode. A realistic procedure is to study the time evolution of bond extensions to understand the collision-induced intramolecular motion of vibrationally excited bonds, the problem which is beyond the normal-mode model. From the dynamics study, we can decide when the C-H distance exceeds a critical value, at which time dissociation is assumed to occur. The occurrence of dissociative events can be readily recognized by studying the time evolution of the methyl (or ring) CH bond trajectory and the CH_{methyl} (or CH_{ring}) vibrational energy, as well as all intermediate modes in the interaction zone, which are conduits for the energy flow. The bond dissociation probability will be defined as the ratio of the number of dissociative trajectories to the total number of trajectories sampled, which is 40,000, in each run.

We define the ensemble-averaged energy transfer $<\Delta E> = <E_{final} - E>$, the difference between the final and initial translational energies of HF. Thus, a positive value of $<\Delta E>$ represents the ensemble-averaged energy loss by toluene, a V $\rightarrow$ T energy transfer process. We also determine the ensemble average of vibrational energy of each mode consisting of kinetic and potential energy terms, and then calculate the difference between this average energy and the energy initially deposited in the mode. The dissociation of a highly excited bond occurs when the bond gains energy from the incident molecule (T $\rightarrow$ V pathway) or it gains energy from adjacent bonds through intramolecular energy flow or both. In any event, the energy gained by the bond must exceed the dissociation threshold, which corresponds to the CH bond extension beyond the point of no return, regardless of the excitation pattern. When the bond dissociation occurs, we need to determine energy transfer for dissociative or nondissociative trajectories separately.

Results and Discussion

A. Dependence of Energy Loss on the Total Vibrational Energy Content. In Figure 3, we show the dependence of energy loss on the total vibrational energy content E_T for θ= 77° at 300 K. The smallest value of E_T considered in this figure is 12,454 cm^{-1} or 1.544 eV, which corresponds to the vibrational energies of C-H_{methyl} and C-H_{ring} being 2274 cm^{-1} (0.282 eV) and 10,180 cm^{-1} (1.262 eV), respectively. That is, both bonds are 3.5 eV below the dissociation threshold of each bond. At this total vibrational energy content, the energy loss is 280 cm^{-1} or 0.0347 eV. Below E_T = 45,000 cm^{-1}, the magnitude of energy loss increases gradually. As shown in Figure 3, for example, when E_T is raised from 12,454 cm^{-1} to 44,700 cm^{-1}, $-<\Delta E>$ increases from 280 cm^{-1} to 938 cm^{-1}, which are nearly 2-8% of E_T. The latter E_T value, 44,700 cm^{-1} corresponds to C-H_{methyl} and C-H_{ring} having the initial vibrational energies of 18,404 cm^{-1} and 26,308 cm^{-1}, respectively, which are 1.5 eV below the dissociation threshold. As the total energy content continues to increase, however, $-<\Delta E>$ now decreases gradually, finally falling to the negative value of –235 cm^{-1} at E_T = 65,680 cm^{-1}. This means that toluene rather gains energy from HF by T $\rightarrow$ V energy transfer when the total vibrational energy content is increased toward the dissociation threshold. In their study on the toluene–N_2 at room temperature,[10] Wright, Sims and Smith found that there is gradual increase in the magnitude of energy loss when the range of the total vibrational energy content is from 500 cm^{-1} to about 40,000 cm^{-1} for toluene excited directly by adsorption of photons at 266 nm. A slow variation of $-<\Delta E>$ with increasing E_T shown in Figure 3 has been known to be the general behavior for the relaxation of toluene by rare gases and diatomic molecules such as N_2 in experimental and theoretical studies.[10,25,30] Furthermore, the experimental work with excited toluene formed via photoisomerization at 308 nm shows the appearance of a maximum value at higher E_T,[10] which is nearly the same E_T at which the maximum appears in the present study.

We also consider the variations of toluene's energy loss with E_T at 200 and 400 K. They are very close to that at 300 K, which means that the temperature dependence is insignificant. Such a weak temperature dependence has already

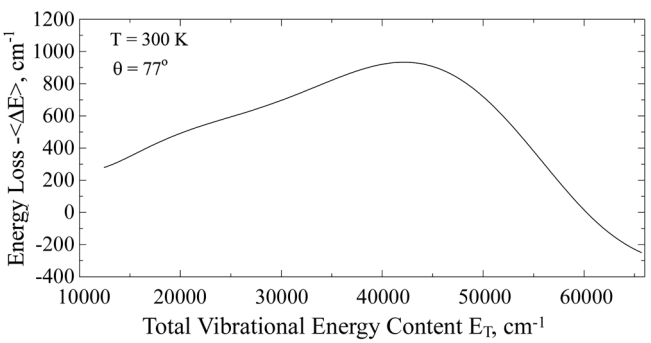

Figure 3. Energy loss against the total vibrational energy content E_T for θ= 77° at T= 300 K.

been noted in experimental studies.[10] Thus, the gross feature of the E_T dependence of $-<\Delta E>$ at these temperatures for the initially excited toluene molecules is that the amount of energy loss increases with increasing vibrational excitation which exhibits weak temperature dependence. The increase of energy loss is weak up to the moderate amount of the vibrational energy content. However, as E_T continues to increase, energy loss decreases gradually and then falls to the negative value when the total vibrational energy content is increased toward the dissociation threshold.

B. Bond Dissociation

Dissociation of C-H_{methyl} versus C-H_{ring}: We now discuss the collision-induced dissociation of highly excited toluene molecules. The possible dissociation pathways of toluene in the present system are

$$C_6H_5CH_3 \rightarrow C_6H_5CH_2 + H_{methyl}, \quad \text{(i)}$$

$$\rightarrow C_6H_4CH_3 + H_{ring}, \quad \text{(ii)}$$

$$\rightarrow C_6H_4CH_2 + H_{methyl} + H_{ring}, \quad \text{(iii)}$$

where Reactions (i) and (ii) produce a radical while Reaction (iii), requiring a greater energy, produces a diradical.

We plot the dissociation probabilities at 300 K for $\theta = 77^o$ in Figure 4. Here we take as before both C-H bonds have their initial vibrational energies which are below their respective dissociation threshold by the same amount. When each of them is 0.9 eV or 7,260 cm^{-1} below the threshold, the total vibrational energy content is 54,390 cm^{-1} above the zero point energy with 31,150 cm^{-1} in C-H_{ring} and 23,240 cm^{-1} in C-H_{methyl}, the dissociation probabilities are $P_{C\text{-}Hmethyl}$ = 0.0009 and $P_{C\text{-}Hring}$ = 0.0004. Here dissociation probabilities are very small because a large amount of energy has to deposit in one of the bonds. We note that the ensemble-averaged energy loss by toluene for E_T = 54,390 cm^{-1} is only 402 cm^{-1} or 0.0498 eV as shown in Figure 3. Since the

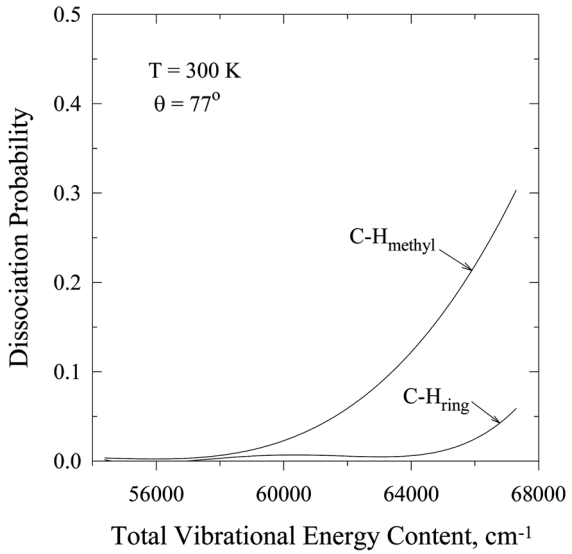

Figure 4. Dissociation probabilities of C-H_{methyl} and C-H_{ring} bonds against the total vibrational energy content E_T for $\theta = 77^o$ at $T = 300$ K.

C-H_{methyl} (or C-H_{ring}) bond is 7,260 cm^{-1} below its dissociation threshold and the molecule loses 402 cm^{-1}, this bond has to gain at least 7,260 cm^{-1} from C-H_{ring} (or C-H_{methyl}) through intramolecular energy redistribution to dissociate. As shown in Figure 4, $P_{C\text{-}Hmethyl}$ is always greater than $P_{C\text{-}Hring}$ for the total vibrational energy content chosen such that both bonds are below their respective dissociation threshold by the same amount of energy at 300 K. When the total energy content is increased from 54,390 cm^{-1} toward the dissociation threshold, the probabilities rise very rapidly. When E_T is as high as 67,294 cm^{-1}, which corresponds to each bond's vibrational energy only 0.1 eV below the dissociation threshold, the dissociation probabilities are now $P_{C\text{-}Hmethyl}$ = 0.2942 and $P_{C\text{-}Hring}$ = 0.060. Such large values indicate that the vibrational motions of a highly excited molecule can be readily perturbed by the incident molecule and need only a small amount of energy to dissociate. In such a highly excited molecule, both C-H bonds can dissociate. In fact, the probability of simultaneous dissociation of C-H_{methyl} and C-H_{ring} is 0.0002, which shows that the majority of dissociative events involve breaking only one C-H bond.

In Figure 5 the dependences of the bond dissociation probability on dissociation time τ are shown for the total energy content E_T = 67,290 cm^{-1}, which corresponds to each bond's vibrational energy only 0.1 eV below the dissociation threshold. To determine the τ-dependent probability $P_{CHmethyl}(\tau)$ (or $P_{CHring}(\tau)$) we have counted the number of trajectories dissociated in each 20 fs interval and recorded it at the mid-point of τ range. For example, the number counted in the 20 fs range between τ = 0.120 ps and 0.140 ps is 592. We then divide this number by 40,000 to obtain $P_{CHmethyl}(\tau)$ = 0.0148 and plot it at the midpoint τ = 0.130 ps. As shown in Figure 5a, the majority of dissociative events of CH_{methyl} bond occur in the short-time range of less than 0.5 ps. The dependence of the dissociation probability $P_{CHmethyl}(\tau)$ on τ in this short time range beyond τ = 0.1 ps is approximately exponential. This exponential behavior is not followed for the dissociative events taking place at τ greater than ≈ 0.5 ps. The dependence beyond this period is flat. However, the distribution of CH_{ring} dissociation probability, closely follow the exponential dependence predicted by RRKM theory[31-33] over the entire dissociation time range beyond τ = 0.5 ps (see Figure 5b). The lifetime distribution for the dissociation of the CH_{methyl} bond in Figure 5a shows that there is no induction period for the bond dissociation, many events occurring in a negligibly short time immediately following the collision with HF. But for the dissociation of the CH_{ring} bond, the distribution takes an induction period of nearly 0.23 ps (see Figure 5b) before sharply rising to the maximum at τ = 0.49 ps and then decaying exponentially. The disparity in the two induction periods represents the situation in which the CH_{methyl} dissociation occurs immediately following the collision, essentially single step, producing rapid T → V energy transfer. On the other hand, the CH_{ring} dissociation occurs following a period of intramolecular vibrational energy flow from CH_{methyl} to the CH_{ring} side

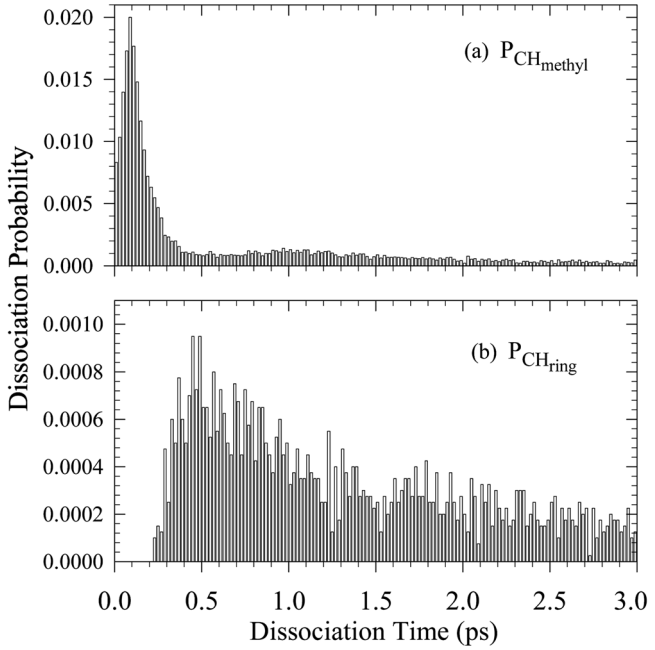

Figure 5. Dependence of the CH dissociation probability on the dissociation time τ for the total vibrational energy content E_T = 67,290 cm^{-1} and θ= 77°. (a) $P_{CHmethyl}$ (b) P_{CHring}.

since direct T → V energy transfer in the HF···CH_{ring} interaction is inefficient.[17]

Energy flow from CH_{methyl} to CH_{ring} is favored over the flow in the reverse direction. This intramolecular energy transfer process is of major importance in dissociating the CH_{ring} bond since T → V energy transfer from HF to CH_{ring} is inefficient as mentioned above. If the CH_{methyl}-to-CH_{ring} energy flow is absent or insignificant, the ring CH dissociation probability would be zero.[17] The energy coming from CH_{methyl} can be either a part of the vibrational energy initially deposited in CH_{methyl} or that transferred from HF or both.

Figure 5a also shows a significant number of the trajectories leads to the CH_{methyl} dissociation at large dissociation time and the dependence of probabilities on dissociation time is not exponential. On the other hand, in the CH_{ring} dissociation dynamics, the exponential dependence extends to the entire time region considered in the study, see Figure 5b. The initial energy content of CH_{methyl} is 29,700 cm^{-1}, whereas that of CH_{ring} is 37,600 cm^{-1}. That is, the higher the initial energy content (or excitation), the closer the dissociation dynamics approaches the statistical behavior. It is important to note that the dissociations occurring at a long time after the start of collision normally follow a complex-mode mechanism,[11] in which the dissociating CH bond near the threshold undergoes a large amplitude motion for a considerable duration before releasing the H atom.[11] This mechanism contrasts the direct-mode mechanism for the short-time events occurring on a subpicosecond time scale. We will consider in detail these two mechanisms in the later section.

In Figure 6, we show the dependence of the dissociation probabilities of C-H bonds on the collision energy for E_T = 67,290 cm^{-1}, which corresponds to each bond's vibrational energy only 0.1 eV below the dissociation threshold. As shown in Figure 6, the dissociation probability of C-H_{methyl} bond is always larger than that of C-H_{ring}. This result is consistent with the result presented in Figure 4 at thermal energies. At E = 2 eV, $P_{C\text{-}Hmethyl}$ is as large as 0.688, whereas $P_{C\text{-}Hring}$ is only 0.066. At such high collision energies, where HF approaches very close to toluene, the incident molecule can maintain a near-collinear alignment with C-H_{methyl} for efficient perturbation (see Figure 2). As can be seen in Figure 2, such alignment is not possible for C-H_{ring} at close range. Furthermore, at such high collision energies, when energy transfer between toluene and HF is large, energy flow to the inner region of the molecule can be important. In particular, the energy initially deposited in the C-H_{ring} vibration will readily flow to this region, when the molecule is strongly perturbed. A low probability of dissociation for C-H_{ring} seen in Figure 6 at high collision energies is due to the initial energy propagating through the C-C bonds and then finally accumulating in the inner region of the molecule, rather than in the C-H_{methyl}.

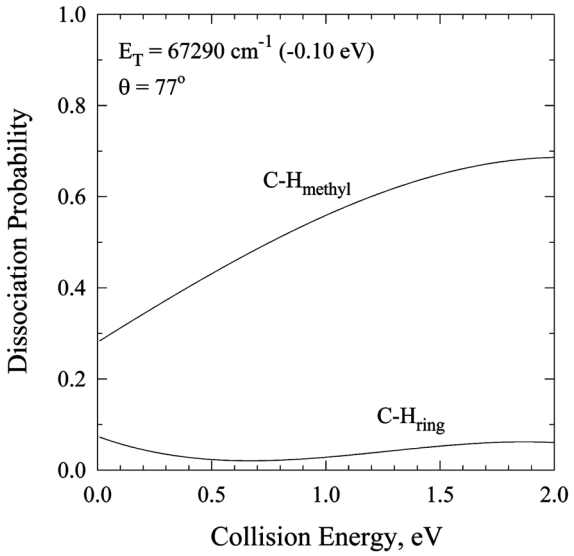

Figure 6. Dissociation probabilities of C-H_{methyl} and C-H_{ring} bonds against the collision energy for the total vibrational energy content E_T = 67,290 cm^{-1} and θ= 77°.

Dynamics of Bond Dissociation: Many C-H dissociative events occur in a direct collision on a subpicosecond time scale, a direct-mode mechanism. Such direct-mode dissociative events for E_T = 60,840 cm^{-1}, which corresponds to each bond's vibrational energy only 0.5 eV below the dissociation threshold, are represented by a typical case shown in Figure 7. We note that the incoming segment of the toluene-HF distance is the collision trajectory and its outgoing segment after reaching the distance of closest approach is the distance between benzyl radical and HF. Intramolecular energy flow between the C-H bonds is seen in Figure 7b, where the time evolution of the vibrational energies of C-H_{methyl} and C-H_{ring} is shown. For this trajectory E = 0.119 eV and toluene transfers 0.051 eV to HF. The

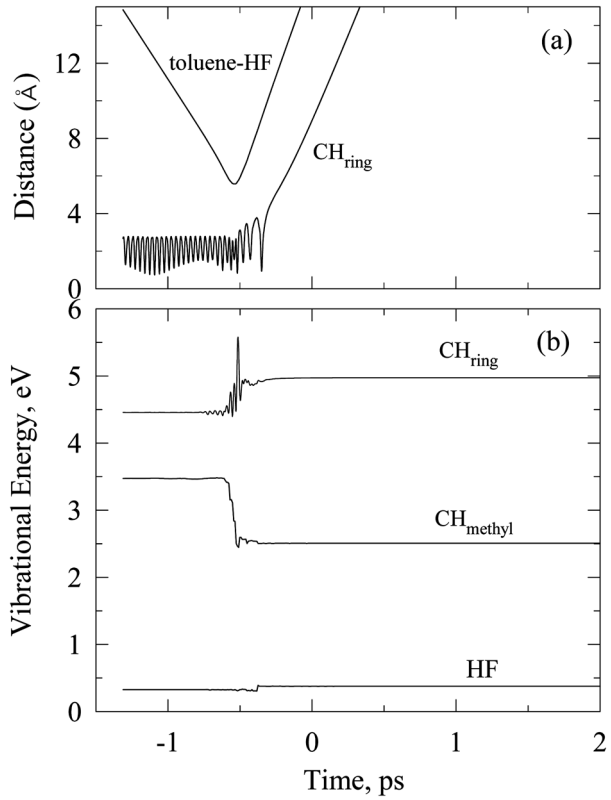

Figure 7. Dynamics of the trajectory representing the C-H$_{ring}$ direct-mode dissociation of toluene with E_T = 60,850 cm^{-1} and θ = 77° at 300 K. (a) Time evolution of the collision and bond trajectory. (b) vibrational energies of C-H$_{ring}$, C-H$_{methyl}$ and HF.

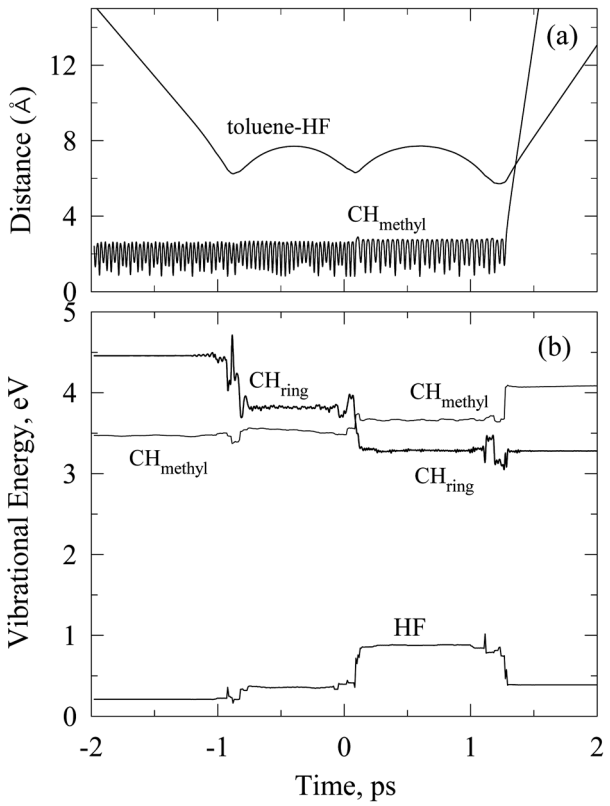

Figure 8. Dynamics of the trajectory representing the C-H$_{methyl}$ complex-mode dissociation of toluene with E_T = 60,850 cm^{-1} and θ = 77° at 300 K. (a) Time evolution of the collision and bond trajectory. (b) vibrational energies of C-H$_{ring}$, C-H$_{methyl}$ and HF.

amount of energy lost by the relaxing C-H$_{methyl}$ is 0.964 eV (see Figure 7b). Thus, the total reaction energy available for intramolecular energy flow is (0.964 eV-0.051 eV) = 0.913 eV. Upon collision with HF, the C-H$_{ring}$ bond takes the bulk of this energy (0.518 eV) and just exceeds the dissociation threshold 4.957 eV. The remaining energy 0.395 eV deposits mainly in the C-C-H$_{ring}$ bend. Although the dissociation of C-H$_{ring}$ is considered here in Figure 7a, C-H$_{methyl}$ dissociation events can be discussed similarly.

There is another class of C-H dissociation, in which the C-H$_{methyl}$ dissociation is not instantaneous. In this complex-mode reaction, HF is trapped on the molecule for a long period, but then redissociates when the C-H$_{methyl}$ bond ruptures. The trajectory representing such events is shown in Figure 8, where the incident molecule becomes trapped to toluene for a period as long as 2 ps – a reaction time which is far longer than that of direct-mode dissociation shown in Figure 7. When the reactive event follows a complex-mode collision, the bonds continue to adjust their energies beyond the initial stage of collision, but the amount involved is small. But toward the end of collision it receives additional energy from the receding HF molecule. For the trajectories considered in Figures 7 and 8, the collision energies are 0.119 and 0.089 eV, respectively. The collisions at a higher incident energy tend to dissociate the C-H bond in the direct-mode mechanism on a subpicosecond time scale, whereas those collisions taking place at a lower energy follow the complex-mode mechanism in which the reaction time can be as long as several picoseconds. Since the average translational energy at 300 K is 0.0387 eV, reactive events are dominated by the collisions in which the incident molecule approaches toluene with energy in the high end tail of the Maxwell distribution.

Concluding Comments

We have studied CH bond dissociation and energy transfer, both intermolecular and intramolecular, in the toluene-HF collision system at 300 K using classical trajectory procedures. The collision system consists of the interaction zone, where the incident molecule interacts with both CH$_{methyl}$ and CH$_{ring}$ bonds, and the inner zone which includes the stretches and bends of toluene beyond the interaction zone.

Energy loss is found to be small, but slowly increases with the total vibrational energy content initially stored in the C-H$_{methyl}$ bond and the adjacent C-H$_{ring}$ bond. Energy loss takes a maximum value as the energy content increases toward the dissociation threshold. Although the extent of energy lost by excited toluene *via* V → T energy transfer is not large, intramolecular vibrational energy flow between the C-H bonds is efficient and takes place on a sub-

picosecond time scale. When the vibrational energies of both C-H bonds are set initially below the dissociation threshold by the same amount, the dissociation probability of C-H_{methyl} bond is found to be larger than that of C-H_{ring} bond. Collision-induced bond dissociation and energy transfer processes in toluene are mainly controlled by the CH_{methyl}-HF interaction. In particular, the CH_{ring}-HF interaction does not produce bond dissociation.

Further excitation of the CH_{methyl} bond toward the dissociation threshold as well as the relaxation of the highly excited CH_{methyl} involve large amounts of energy transfer ($>> k_BT$) occurring essentially in single-step processes in strong collisions. The CH_{methyl} bond dissociation occurs without an induction period. The dissociation of the highly excited CH_{ring} bond is a result of intramolecular energy flow from CH_{methyl} with the CH_{ring} bond acquiring its energy for dissociation in a series of small steps over a period longer than 0.5 ps. Unlike the CH_{methyl} dissociation, this reaction thus occurs after a considerable induction period. While many dissociative events occur immediately following the intramolecular energy flow step on a subpicosecond time scale in a direct-mode mechanism, a significant fraction of reactive events occurs many picoseconds after the start of collision. In such events, the incident atom becomes trapped on the molecule undergoing a large amplitude motion during the complex-mode collision.

Acknowledgments. This work was financially supported by research fund of Chonnam National University in 2003. The computational part of this work was supported by "the 6th Supercomputing Application Support Program" of the KISTI (Korea Institute of Science and Technology Information).

References

1. Cottrell, T. L.; McCoubrey, J. C. *Molecular Energy Transfer in Gases*; Butterworths: London, 1961; experimental data in Ch. 5 and review of theoretical approaches in Ch. 6.
2. *Transfer and Storage of Energy by Molecules, Vol.* 2; Burnett, G. M.; North, A. M., Eds.; Wiley: New York, 1969.
3. Smith, I. W. M. In *Gas Kinetics and Energy Transfer, Vol. 2*, Specialist Periodical Reports; Chemical Society, Burlington House: London, 1977; pp 1-57.
4. Yardley, J. T. *Introduction to Molecular Energy Transfer*; Academic: New York, 1980.
5. Lendvay, G.; Schatz, G. C. *J. Phys. Chem.* **1990**, *94*, 8864; **1994**, *98*, 6530; Lendvay, G.; Schatz, G. C. *J. Chem. Phys.* **1993**, *98*, 1034; Lendvay, G.; Schatz, G. C.; Harding, L. B. *Faraday Discuss.* **1995**, *102*, 389.
6. Toselli, B. M.; Barker, J. R. *J. Chem. Phys.* **1992**, *97*, 1809.
7. Clarke, D. L.; Oref, I.; Gilbert, R. G. *J. Chem. Phys.* **1992**, *96*, 5983.
8. Clary, D. C.; Gilbert, R. G.; Bernshtein, V.; Oref, I. *Faraday Discuss.* **1995**, *102*, 423.
9. Sevy, E. T.; Rubin, S. M.; Lin, Z.; Flynn, G. W. *J. Chem. Phys.* **2000**, *113*, 4912.
10. Wright, S. M. A.; Sims, I. R.; Smith, I. W. M. *J. Phys. Chem. A* **2000**, *104*, 10347.
11. Ree, J.; Kim, Y. H.; Shin, H. K. *J. Chem. Phys.* **2002**, *116*, 4858.
12. Lim, K. F. *J. Chem. Phys.* **1994**, *101*, 8756.
13. Catlett, D. L. Jr.; Parmenter, C. S.; Pursell, C. J. *J. Phys. Chem.* **1994**, *98*, 3263; *J. Phys. Chem.* **1995**, *99*, 7371.
14. Shin, H. K. *J. Phys. Chem. A* **1999**, *103*, 6030.
15. Shin, H. K. *J. Phys. Chem. A* **2000**, *104*, 6699.
16. Nilsson, D.; Nordholm, S. *J. Chem. Phys.* **2002**, *116*, 7040.
17. Ree, J.; Kim, Y. H.; Shin, H. K. *Chem. Phys. Lett.* **2004**, *394*, 250.
18. Ree, J.; Chang, K. S.; Kim, Y. H.; Shin, H. K. *Bull. Korean Chem. Soc.* **2003**, *24*, 1223; Ree, J.; Kim, Y. H.; Shin, H. K. *Bull. Korean Chem. Soc.* **2005**, *26*, 1269.
19. Yerram, M. L.; Brenner, J. D.; King, K. D.; Barker, J. R. *J. Phys. Chem.* **1990**, *94*, 6341.
20. Damm, M.; Hippler, H.; Olschewski, H. A.; Troe, J.; Willner, J. *Z. Phys. Chem.* **1990**, *166*, 129.
21. Toselli, B. M.; Brenner, J. D.; Yerram, M. L.; Chin, W. E.; King, K. D.; Barker, J. R. *J. Chem. Phys.* **1991**, *95*, 176.
22. Damm, M.; Deckert, F.; Hippler, H.; Troe, J. *J. Phys. Chem.* **1991**, *95*, 2005.
23. Lenzer, T.; Luther, K.; Troe, J.; Gilbert, R. G.; Lim, K. F. *J. Chem. Phys.* **1995**, *103*, 626.
24. Hirschfelder, J. O.; Curtiss, C. F.; Bird, R. B. *Molecular Theory of Gases and Liquids*; Wiley: New York, 1967; see p 168 for the combining laws, pp 1110-1112 and 1212-1214 for D and σ.
25. Lim, K. F. *J. Chem. Phys.* **1994**, *100*, 7385.
26. Huber, K. P.; Herzberg, G. *Constants of Diatomic Molecules*; Van Nostrand Reinhold: New York, 1979.
27. Xie, Y.; Boggs, J. E. *J. Comp. Chem.* **1986**, *7*, 158.
28. Gear, C. W. *Numerical Initial Value Problems in Ordinary Differential Equations*; Prentice-Hall: New York, 1971.
29. MATH/LIBRARY, *Fortran Subroutines for Mathematical Applications*; IMSL: Houston, 1989; p 640.
30. Shi, J.; Barker, J. R. *J. Chem. Phys.* **1988**, *88*, 6219.
31. Bunker, D. L. *Theory of Elementary Gas Reaction Rates*; Pergamon: London, 1966.
32. Peslherbe, G. H.; Hase, W. L. *J. Chem. Phys.* **1994**, *101*, 8535.
33. Steinfeld, J. I.; Francisco, J. S.; Hase, W. L. *Chemical Kinetics and Dynamics*, 2nd ed; Prentice Hall: Englewood Cliffs, NJ, 1998; pp 362-367.